Influence of Ti doping on galvanomagnetic properties and valence band energy spectrum of $Sb_{2-x}Ti_xTe_3$ single crystals

1999 J. Phys.: Condens. Matter 11 5273

(http://iopscience.iop.org/0953-8984/11/27/304)

J. Phys.: Condens. Matter **11** (1999) 5273–5282. Printed in the UK PII: S0953-8984(99)01999-2

Influence of Ti doping on galvanomagnetic properties and valence band energy spectrum of $Sb_{2-x}Ti_xTe_3$ single crystals

V A Kulbachinskii†, N Miura‡‖, H Nakagawa‡, C Drashar§ and P Lostak§

† Low Temperature Physics Department, Moscow State University, 119899 Moscow, Russia
‡ Institute of Solid State Physics, University of Tokyo, Roppongi, Minato-ku, Tokyo, Japan
§ University of Pardubice, 53210, Pardubice, Czech Republic

E-mail: miura@issp.u-tokyo.ac.jp

Received 19 February 1999

Abstract. The Shubnikov–de Haas (SdH) effect in $Sb_{2-x}Ti_xTe_3$ single crystals was investigated as a function of Ti content for $0 < x < 0.02$ at $T = 4.2$ K in high magnetic fields up to 40 T applied along the c_3-axis. We found that by doping Ti into Sb_2Te_3, the cross-section of the six-ellipsoidal Fermi surfaces of the upper valence band decreases. For Ti content $x > 0.001$ we observed the second frequency of the SdH oscillations associated with the lower valence band. The second frequency decreased with increasing x. From the temperature dependence of the resistivity and the Hall effect in the temperature range $4.2 < T < 300$ K, it was found that the increase of Ti content suppresses the initial hole concentration. Parameters of the crystal lattice and thermopower were measured at room temperature as a function of Ti content.

1. Introduction

Antimony telluride Sb_2Te_3 belongs to layered compounds with the same tetradymite structure as Bi_2Te_3. It usually involves anti-site defects (the occurrence of Sb atoms occupying Te lattice sites). Due to such native defects, Sb_2Te_3 shows always a p-type conductivity with the hole concentration up to 10^{20} cm^{-3}. The Fermi surface of the upper valence band in Sb_2Te_3 consists of six ellipsoids, tilted from the normal to the basal plane [1]. Such a Fermi surface corresponds to the Drabble–Wolf model [2]. The value of the tilted angle θ is not known exactly, but according to interpolation to $x = 1$ in $(Bi_{1-x}Sb_x)_2Te_3$, θ is estimated to be about 50° [3]. von Middendorf *et al* reported that the energy separation between the extrema of the upper valence band (UVB) and the lower valence band (LVB) should be 150 meV [1], but this value seems to be too large. It is considered to be of the order of 20–30 meV because that for $(Bi_{1-x}Sb_x)_2Te_3$ ($0 < x < 1$) is about 30 meV [3]. Sb_2Te_3 based solid solutions have been studied by several authors [4–7]. For example, the plasma frequency at room temperature [4], the lattice parameters and the conductivity at room temperature [5] have been measured for $In_xSb_{2-x}Te_3$. In experiments on the Shubnikov–de Haas (SdH) effect and the transient thermoelectric effect measurements [6, 7] for $In_xSb_{2-x}Te_3$ ($0 \leqslant x \leqslant 0.4$) and $Sb_2Te_{3-y}Se_y$ ($0 \leqslant y \leqslant 1.8$) single crystals, we obtained evidence for the existence of the lower lying second six-ellipsoidal valence bands with heavy effective masses. In or Se doping decreases the hole concentration in $In_xSb_{2-x}Te_3$ and $Sb_2Te_{3-y}Se_y$ due to suppression of the anti-site defects which are responsible for the high initial concentration of holes in Sb_2Te_3.

‖ Author to whom correspondence should be addressed.

0953-8984/99/275273+10$30.00

For further understanding the properties of Sb_2Te_3 based solutions, we have carried out measurements of dc conductivity in the temperature range 4.2–300 K, and the SdH effect at a temperature 4.2 K in magnetic fields up to 40 T in $Sb_{2-x}Ti_xTe_3$ ($0 \leqslant x \leqslant 0.02$) single crystals. We focus on the effect of Ti substitution into the host Sb_2Te_3 crystal to obtain information on the valence band structure.

2. Sample preparation and experiments

For preparing $Sb_{2-x}Ti_xTe_3$ single crystals, polycrystalline Sb, Te of 5 N purity and $TiTe_2$ compound were used. The synthesis of the polycrystalline $TiTe_2$ compound was carried out by heating a stoichiometric mixture of Ti and Te powder in an evacuated silica ampoule at 1100 °C for 5 days. In the second step, Ti doped polycrystalline material was prepared from the mixture of Sb, Te and $TiTe_2$, corresponding to the atomic ratio (Sb + Ti)/Te = 2/3 in evacuated silica ampoules. The synthesis was carried out in a horizontal furnace at $T \sim 773$ °C for 48 hours. The single crystals were grown by the modified Bridgman method: conical ampoules with the polycrystalline material were placed into the upper part of a Bridgman furnace with a higher temperature where they were heat treated at 700 °C for 24 hours. Then the ampoule was lowered in the temperature gradient of 400 K cm^{-1} at a rate of 1.3 mm h^{-1}.

The crystals were easily cleaved perpendicular to the trigonal c_3-axis, i.e. along the (0001) plane which was parallel to the ampoule axis. The Ti contents in the mixed crystals were determined by x-ray microprobe analysis and atomic absorption spectrometry. Samples for transport measurements were cut from cleaved single crystal plates by a spark erosion machine (typical dimensions: $5 \times 1 \times 0.5$ mm^3). The lattice parameters of the samples are listed in table 1. It was found that both lattice parameters a and c as well as the unit cell volume decrease as the Ti concentration increases.

Table 1. Lattice parameters a, c and volume of the unit cell V of $Sb_{2-x}Ti_xTe_3$ single crystal at room temperature.

x	Concentration of Ti (10^{19} cm^{-3})	a (nm)	c (nm)	V (nm^3)
0	0	0.426 48(3)	3.0450(1)	0.479 64(6)
0.001	0.14	0.426 57(4)	3.0443(2)	0.479 73(9)
0.007	0.97	0.426 49(3)	3.0440(2)	0.479 50(7)
0.01	6.2	0.426 41(4)	3.0438(2)	0.479 30(9)
0.02	10.1	0.426 35(3)	3.0441(2)	0.479 20(7)
0.04	19.0	0.426 33(3)	3.0440(2)	0.479 14(8)

For investigating the SdH effect in high magnetic fields, we used pulse magnets which can produce pulsed fields up to 40 T with a duration time of about 20 ms. The resistivity and the Hall effect were measured by a potentiometric method with a dc current along the c_2-direction in magnetic fields up to 7 T applied along the c_3-axis (perpendicular to the layers) using a superconducting magnet.

3. Experimental results

3.1. Transport measurement

In table 2, we list the resistivity ρ, the Hall mobility μ and the Hall coefficient R_H at different temperatures for the samples of $Sb_{2-x}Ti_xTe_3$. Figure 1 shows the temperature

Table 2. Resistivity ρ, Hall mobility μ and Hall coefficient R_H at different temperatures for $Sb_{2-x}Ti_xTe_3$.

x	$\rho^{4.2}$ (mΩ cm)	ρ^{300} (mΩ cm)	$R_{\tilde{o}}^{4.2}$ (cm^3 C^{-1})	R_x^{77} (cm^3 C^{-1})	$R_{\tilde{o}}^{300}$ (cm^3 C^{-1})	$\mu_x^{4.2}$ (m^2 V^{-1} s^{-1})	μ_x^{300} (m^2 V^{-1} s^{-1})
0	0.031	0.25	0.059	—	0.0865	0.19	0.035
0.001	0.034	0.27	0.082	—	0.080	0.24	0.030
0.003	0.043	0.30	0.094	—	0.080	0.22	0.027
0.007	0.076	0.34	0.090	0.089	0.170	0.12	0.050
0.01	0.11	0.43	0.091	—	0.220	0.08	0.051
0.013	0.26	0.55	0.092	0.089	0.240	0.035	0.044
0.019	0.66	1.19	0.098	—	—	0.014	—
0.02	0.35	0.83	0.13	0.11	0.360	0.038	0.044

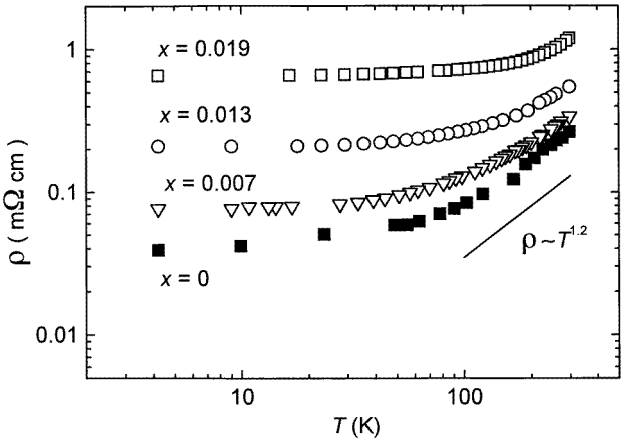

Figure 1. Temperature dependence of resistivity in logarithmic scales for $Sb_{2-x}Ti_xTe_3$ samples with different x.

dependence of the resistivity ρ for $Sb_{2-x}Ti_xTe_3$ ($0 < x < 0.02$) along the c_2-axis. For all samples, ρ decreases with decreasing temperature and then approaches a constant value at low temperatures. Residual resistivity increases with increasing substitution of Ti atoms. In the temperature range 77–300 K, the ρ–T curves obey a power law of the form $\rho = T^m$ with the exponents $m \sim 1.2$ for all samples. As is well known, $m = 1.5$ corresponds to acoustic phonon scattering. A slight deviation from $m = 1.5$ for $Sb_{2-x}Ti_xTe_3$ is due to additional scattering by ionized impurities and the temperature dependence of the effective mass.

The Hall coefficient R_H is positive for all samples and is found to be temperature dependent in the whole temperature range 4.2–300 K. The values of R_H and the Hall mobility $\mu_H = R_H\sigma$ at 4.2 K are plotted against the Ti content x for $Sb_{2-x}Ti_xTe_3$ in figures 2 and 3, respectively. The Hall coefficient increases monotonically at room temperature with increasing concentration of Ti, which indicates that the apparent hole concentration decreases with increase of x. On the other hand, the Hall coefficient decreases when temperature is lowered down to 77 K and then slightly increases. The Hall mobility μ_H at $T = 4.2$ K decreases with increasing x for $Sb_{2-x}Ti_xTe_3$ but not so drastically as for $In_xSb_{2-x}Te_3$ [6]. At room temperature for Ti content $x < 0.013$, the Hall mobility even increases with x. One of the reasons is the change in the carrier scattering as was observed in Bi_2Te_3 [8].

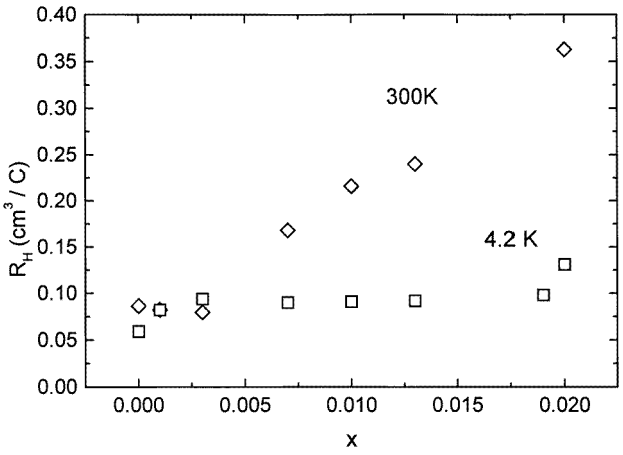

Figure 2. Dependence of the Hall coefficient R_H at 300 and 4.2 K on Ti concentration x.

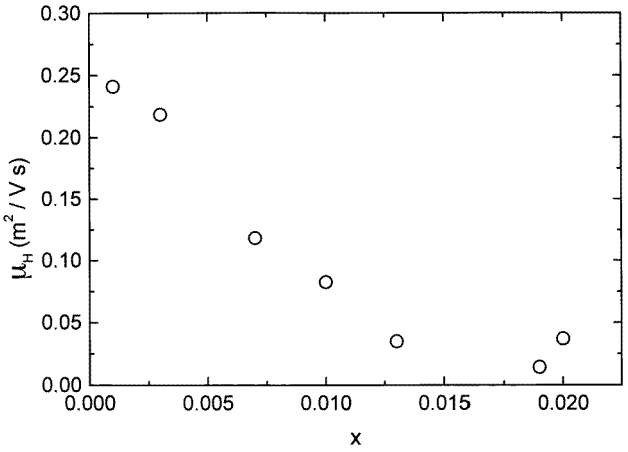

Figure 3. Dependence of the Hall mobility μ_H at $T = 4.2$ K on Ti concentration x.

3.2. Shubnikov–de Haas effect

In low magnetic fields, the magnetoresistance of the samples is proportional to B^2 as expected. In higher magnetic fields, we can observe the SdH oscillation in Sb_2Te_3 and $Sb_{2-x}Ti_xTe_3$. In figure 4, the SdH oscillation of the transverse magnetoresistance is shown for different samples of $Sb_{2-x}Ti_xTe_3$ in magnetic fields parallel to the c_3-axis of the crystal. Here the monotonic part of the background is subtracted. In this orientation, the extremal cross-sections of all the ellipsoids of the six Fermi surfaces of the upper valence band coincide. We observed only a single frequency in Sb_2Te_3 up to the highest magnetic field of about 40 T. Due to decrease of the mobility in the $Sb_{2-x}Ti_xTe_3$ system with increasing Ti content, the amplitude of the oscillation falls with x. For $x = 0.02$ it is already difficult to detect the SdH effect in magnetic fields up to 40 T. Fast Fourier transform data are shown in figure 5. As is seen in figures 4 and 5, a new high frequency F_2 appears in the SdH oscillations for $x > 0.001$. The values of the both frequencies decrease as the Ti content x increases.

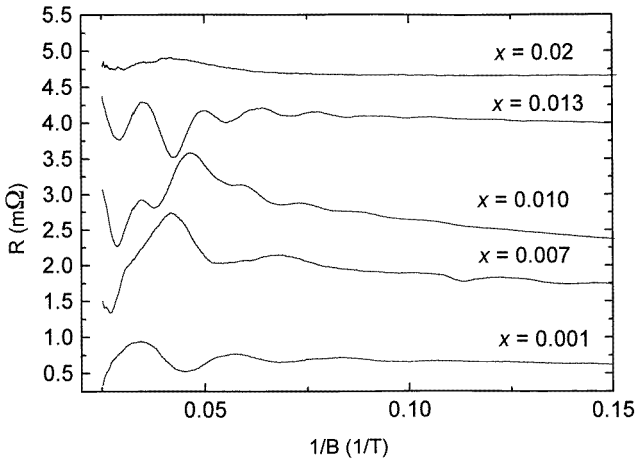

Figure 4. Oscillating part of the SdH oscillations against inverse magnetic field B at $T = 4.2$ K of $Sb_2Ti_xTe_3$ single crystals with different x.

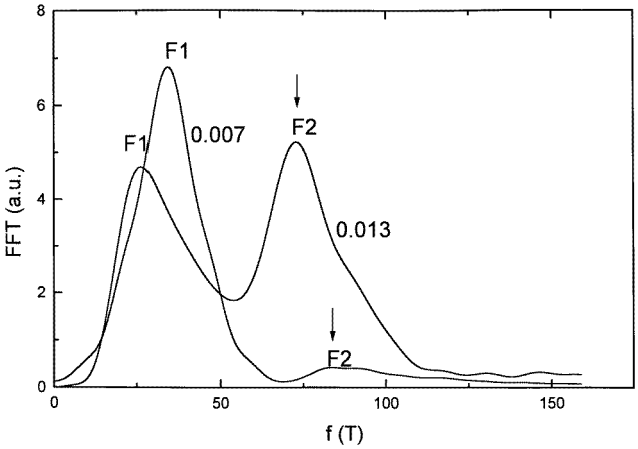

Figure 5. The Fourier transforms of the SdH oscillations of $Sb_2Ti_xTe_3$ for two samples with $x = 0.007$ and $x = 0.013$. Arrows mark the second higher frequency.

In figure 6 we plot the dependence of the lower and higher frequencies F_1 and F_2 on Ti content x. The appearance of a new frequency F_2 is ascribed to the lower lying second valence band. The existence of the second valence band is evident also from the temperature dependence of the Hall coefficient as discussed later.

4. Discussion

4.1. Shubnikov–de Haas effect

Several studies have been made on the valence band of Sb_2Te_3, $(Sb_{1-x}Bi_x)_2Te_3$ and other mixed crystals of this type [1–7]. From the SdH data obtained on p-type $(Sb_{1-x}Bi_x)_2Te_3$ crystals with $0 < x < 1$, we have confirmed that the six-ellipsoidal model is valid for the

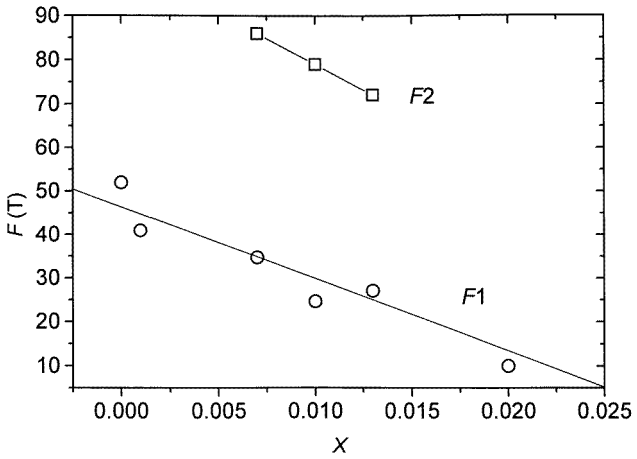

Figure 6. The Ti concentration dependence of the main SdH frequency F_1 and additional frequency F_2 at $\boldsymbol{B}$ parallel to c_3 for $Sb_2Ti_xTe_3$.

highest valence band in these crystals. From some experimental data it is also evident that there exist the second lowest valence bands with six-ellipsoidal constant energy surfaces [6, 7]. For quantitative comparison between the Hall effect and the SdH data, it is necessary to know the anisotropy of the Fermi surface. However, we have not made measurement with an angle corresponding to the maximum cross-section of the Fermi surface. Therefore, we calculate the carrier concentration in the six ellipsoids from the SdH data, and compare it with the Hall effect data. The ellipsoidal non-parabolic band model satisfactorily describes the energy spectrum of holes in the highest valence band of Sb_2Te_3 [1–3]. The dispersion relation in this model can be represented in the following form

$$2m_0E = \hbar^2(\alpha_{11}k_1^2 + \alpha_{22}k_2^2 + \alpha_{33}k_3^2 + 2\alpha_{23}k_2k_3) \tag{1}$$

where $\alpha_{ij} = m_0/m_{ij}$ are the energy dependent inverse mass tensor components, and k_1, k_2 and k_3 are the Cartesian co-ordinates in the $\boldsymbol{k}$-space, parallel to one of the binary, bisectrix, and trigonal axes, respectively. The period of the oscillation in this model is related to the parameters α_{ij} as

$$\Delta(1/B) = e\hbar/m_0E_F[(\alpha_{22}\alpha_{33} - \alpha_{23}^2)\cos^2\alpha + \alpha_{11}\alpha_{33}\cos^2\beta + \alpha_{11}\alpha_{22}\cos^2\gamma + 2\alpha_{11}\alpha_{23}\cos\beta\cos\gamma]^{1/2}. \tag{2}$$

Here the $\cos\alpha$, $\cos\beta$ and $\cos\gamma$ are the direction cosines of B in the $\boldsymbol{k}$-space.

Let us take one ellipsoid as shown in figure 7. The main axis of the ellipsoid is denoted as a, b, c, and the extremal cross-sections as S_a, S_b, S_c respectively. S_H is the cross-section of the Fermi surface for $\boldsymbol{B}$ parallel to the c_3-axis. The value of S_H can be determined from the frequency of the SdH oscillation $F = \Delta[(1/B)]^{-1}$

$$S_H = 2\pi e[\hbar\Delta(1/B)]^{-1}. \tag{3}$$

The principal axis of the six ellipsoids is tilted by an angle θ in the mirror plane from the c_2-axis

$$k_1 = k_1' \qquad k_2 = k_2'\cos\theta - k_3'\sin\theta \qquad k_3 = k_2'\sin\theta + k_3'\cos\theta. \tag{4}$$

The constant energy surfaces are commonly described by

$$2m_0E/\hbar^2 = \alpha_{11}'(k_1')^2 + \alpha_{22}'(k_2')^2 + \alpha_{33}'(k_3')^2 \tag{5}$$

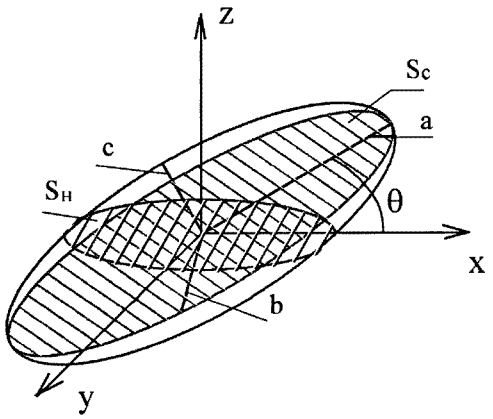

Figure 7. Single ellipsoid of the Fermi surface with some important cross-sections.

where

$$\alpha'_{22}+\alpha'_{33}=\alpha_{22}+\alpha_{33} \qquad \alpha'_{22}\alpha'_{33}=\alpha_{22}\alpha_{33}-(\alpha_{23})^2 \qquad \tan 2\theta=-2\alpha_{23}/(\alpha_{22}+\alpha_{33}). \quad (6)$$

Thus the principal axes of ellipsoids are equal to:

$$a=(2m_0E_F/\alpha'_{11})^{1/2}/\hbar \qquad b=(2m_0E_F/\alpha'_{22})^{1/2}/\hbar \qquad c=(2m_0E_F/\alpha'_{33})^{1/2}/\hbar. \quad (7)$$

Then

$$\begin{aligned} S_a &= \pi cb = 2\pi m_0E_F/(\alpha'_{22}\alpha'_{33})^{1/2}\hbar^2 \\ S_b &= \pi ac = 2\pi m_0E_F/(\alpha'_{11}\alpha'_{33})^{1/2}\hbar^2 \\ S_c &= \pi ab = 2\pi m_0E_F/(\alpha'_{11}\alpha'_{22})^{1/2}\hbar^2. \end{aligned} \quad (8)$$

Referring to figure 7, it can be readily shown that

$$S_H=[(\cos\varphi/S_a)^2+(\sin\varphi/S_c)^2]^{-1/2} \quad (9)$$

where $\varphi=\pi/2-\theta$ and

$$S_H=2\pi m_0E_F/(\alpha'_{22}\alpha'_{33}\sin^2\theta+\alpha'_{11}\alpha'_{22}\cos^2\theta)^{1/2}\hbar^2. \quad (10)$$

The volume of one ellipsoid is given by

$$\begin{aligned} V=4\pi abc/3=4(S_aS_bS_c/\pi)^{1/2}/3=[4/3(\pi)^{1/2}][S_H(\alpha'_{22}\alpha'_{33}\sin^2\theta \\ +\alpha'_{11}\alpha'_{22}\cos^2\theta)^{1/2}]^{3/2}/(\alpha'_{11}\alpha'_{22}\alpha'_{33})^{1/2}. \end{aligned} \quad (11)$$

The concentration of holes p in all six ellipsoids is

$$p=6\times 2V/(2\pi\hbar)^3. \quad (12)$$

To calculate the hole concentration in the upper band p_{1SdH} we took the tilt angle of ellipsoids to the basal plane as about 48° obtained by extrapolating to $x=1$ for $(Bi_{1-x}Sb_x)_2Te_3$ crystals [2]. We calculated the hole concentration in $Sb_{2-x}Ti_xTe_3$ crystals and its dependence on x under an assumption that the anisotropy of the Fermi surface and the tilt angles of ellipsoids do not depend on x. The band edge parameters were taken as $\alpha'_{11}=2.26$, $\alpha'_{22}=32.5$, $\alpha'_{33}=11.6$ [2]. The calculated results are listed in table 3. If only the frequency F_1 is taken for calculations, the SdH concentration is always less then the Hall concentration $1/eR_H$. This fact gives an evidence for the existence of the second lower valence band. Indeed, in the SdH effect we observed at $\boldsymbol{B}$ parallel to the c_3-axis for $x>0.001$ two different frequencies of

oscillations in $Sb_{2-x}Ti_xTe_3$ crystals. The second frequency F_2 is ascribed to the second lower valence band. According to the previous experimental data [6], we can assume that the second lower valence band is also six ellipsoidal. Based on such an assumption, we calculated the hole concentration p_{2SdH} for the frequency F_2 of the SdH effect for $\boldsymbol{B}$ parallel to the c_3-axis using the same procedure and the same parameters as for the upper valence band. The data are summarized in table 3. As seen in table 3, the total hole concentrations in both bands are in good agreement with the value of $1/eR_H$ except for the maximum Ti content. The discrepancy for the maximum Ti content probably comes from the anisotropy of the Fermi surface, which we kept constant but actually depends on carrier concentration.

Table 3. SdH oscillation frequency for $\boldsymbol{B} \parallel c_3$-axis $F_1 = [\Delta(1/B)]^{-1}$ and $F_2 = [\Delta(1/B)]^{-1}$, the value $1/eR_H$ at $T = 4.2$ K and thermopower α^{300} at $T = 300$ K for different $Sb_{2-x}T_xTe_3$.

x	F_1 (T)	F_2 (T)	p_{1SdH} (10^{19} cm^{-3})	p_{2SdH} (10^{19} cm^{-3})	$1/eR_H$ (10^{19} cm^{-3})	α^{300} (μV K^{-1})
0	52		2.2		10.5	92
0.001	41		1.6		7.56	80
0.003					6.6	—
0.007	34.7	86	1.2	4.7	6.88	100
0.01	25	78.5	0.74	4.1	6.81	95
0.013	27	72.7	0.83	3.7	6.74	94
0.019		—	—		6.32	—
0.02	10	—	0.19		4.76	99

4.2. Temperature dependence of the Hall coefficient

The existence of the second valence band is also evident from the temperature dependence of the Hall coefficient R_H, which decreases when temperature decreases down to 77 K and then slightly increases (see table 2). In the case of one degenerate type of carrier such a behaviour leads to paradoxical increase of the hole concentration during cooling according to the simple Hall expression

$$R_H = A/pe \tag{13}$$

where A is the Hall factor. For two different groups of carriers, one has to use more complicated expressions [1, 2, 6, 7]

$$R_x = \sigma_{xy}/\{B(\sigma_{xx}^2 + \sigma_{xy}^2)\} \tag{14}$$

$$\rho = \sigma_{xx}/(\sigma_{xx}^2 + \sigma_{xy}^2) \tag{15}$$

where ρ is resistivity, $\boldsymbol{B}$ is magnetic field, σ_{xx}, σ_{xy} are components of the conductivity tensor:

$$\sigma_{xx} = ep_{lh}\mu_{lh}/\{1 + (\mu_{lh}B)^2\} + ep_{hh}\mu_{hh}/\{1 + (\mu_{hh}B)^2\} \tag{16}$$

$$\sigma_{xy} = ep_{lh}\mu_{lh}(\mu_{lh}B)/\{1 + (\mu_{lh}B)^2\} + ep_{hh}\mu_{hh}(\mu_{hh}B)/\{1 + (\mu_{hh}B)^2\} \tag{17}$$

where μ_{lh}, μ_{hh} are conductivity tensor components, μ_{lh}, μ_{hh} are mobility, and p_{lh}, p_{hh} are concentrations for light and heavy holes respectively (we call the upper valence band holes 'light' and the lower valence band holes 'heavy').

Making use of expressions (14)–(17), the temperature dependence of the Hall coefficient can be satisfactorily fitted to the experimental results. In figure 8 we plot the experimentally observed T dependence of the R_H for a sample $Sb_{1.993}Ti_{0.007}Te_3$ (symbols) as compared with a theoretical curve (solid line) using the following approximation. According to measurements

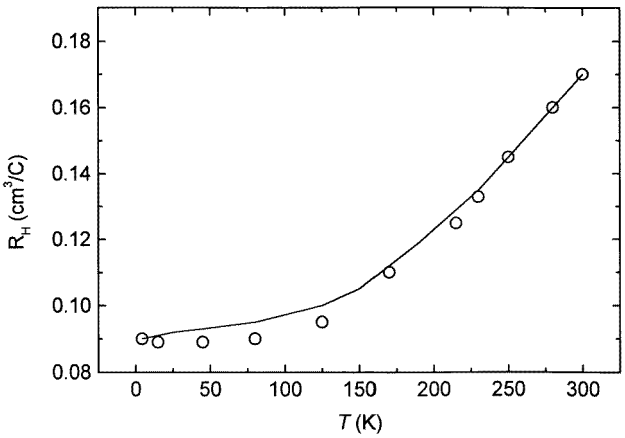

Figure 8. Temperature dependence of the Hall coefficient R_H for sample $Sb_2Ti_xTe_3$ with $x = 0.007$. Symbols are experimental values, the solid line is the fitting for two groups of carriers.

$R_H^{300} = 0.17$ cm^3 C^{-1}, $R_H^{4.2} = 0.09$ cm^3 C^{-1}, $\rho^{4.2} = 0.076$ mΩ cm, $\mu_H^{4.2} = 0.12$ m^2 V^{-1} C^{-1} (see table 1), the SdH concentration is equal to $p_{1SdH} = 1.5 \times 10^{19}$ cm^{-3}.

In this fitting procedure, we took $p_{lh} = p_{1SdH}$ and $\mu_{lh} = \mu_x^{4.2}$, at $T = 4.2$ K assuming that the SdH concentration corresponds to the light holes in the upper valence band, and values p_{hh} and μ_{hh} were calculated from (14)–(17) with the experimental values of $R_H^{4.2}$ and $\rho^{4.2}$. We obtained $p_{hh} = 24 \times 10^{19}$ cm^{-3} and $\mu_{hh} = 0.009$ m^2 V^{-1} s^{-1}. Then we consider that the mobility of the light and heavy holes increases as the temperature is lowered while their concentrations are temperature independent. Thus the anomalous decrease of the Hall coefficient with decreasing temperature is interpreted in terms of the two types of hole in $Sb_2Ti_xTe_3$.

The non-parabolicity of the energy spectrum in Sb_2Te_3 based materials connected preferentially with the second extrema, situated lower by approximately 30 meV than the top of the first valence band. The increase of the Ti content may slightly change the energy gap in $Sb_{2-x}Ti_xTe_3$, but the anisotropy of the Fermi surface and the tilt angles of the ellipsoids cannot change drastically as compared with Sb_2Te_3.

5. Conclusions

The transport and the SdH effect measurements have revealed that (1) in $Sb_2Ti_xTe_3$ single crystals, the hole concentration is decreased by Ti doping; (2) a second frequency in the SdH effect appears in $Sb_2Ti_xTe_3$ for $x > 0.001$ which is ascribed to the second valence band; (3) unusual temperature dependence of the Hall coefficient in low magnetic fields is quantitatively described by the temperature dependence of the mobility in two different six-ellipsoidal valence bands.

Acknowledgment

One of the authors (VAK) would like to thank the JSPS for support during his stay at ISSP University of Tokyo.

References

[1] von Middendorf A, Dietrich K and Lanwehr G 1973 *Solid State Commun.* **3** 443
[2] Drable J R and Wolf R 1956 *Proc. R. Soc.* **69** 1101–8
[3] Kohler H and Freudenberger A 1977 *Phys. Status Solidi* b **195** 195
Kohler H and Freudenberger A 1977 *Phys. Status Solidi* b **195** 195
[4] Horak J, Cernak K and Koudelka L J 1986 *J. Phys. Chem. Solids* **47** 805
[5] Horak J, Lostak P and Benes L 1984 *Phil. Mag.* B **50** 665
[6] Kulbachinskii V A, Dashevskii Z M, Inoue M, Sasaki M, Negishi H, Gao W X, Lostak P, Horak J and de Visser A 1995 *Phys. Rev.* B **52** 10 915
[7] Kulbachinskii V A, Inoue M, Sasaki M, Negishi H and Gao W X 1995 *Proc. 14th Int. Conf. on Thermoelectrics (St. Petersburg)* p 151
[8] Kulbachinskii V A, Negishi H, Sasaki M, Giman Y, Inoue M, Lostak P and Horak J 1997 *Phys. Status Solidi* b **199** 505